



Transgenic Inhibition of Synaptic Transmission Reveals Role of CA3 Output in Hippocampal Learning

Toshiaki Nakashiba, *et al.*
Science **319**, 1260 (2008);
DOI: 10.1126/science.1151120

The following resources related to this article are available online at www.sciencemag.org (this information is current as of March 10, 2008):

Updated information and services, including high-resolution figures, can be found in the online version of this article at:

<http://www.sciencemag.org/cgi/content/full/319/5867/1260>

Supporting Online Material can be found at:

<http://www.sciencemag.org/cgi/content/full/1151120/DC1>

A list of selected additional articles on the Science Web sites **related to this article** can be found at:

<http://www.sciencemag.org/cgi/content/full/319/5867/1260#related-content>

This article **cites 33 articles**, 9 of which can be accessed for free:

<http://www.sciencemag.org/cgi/content/full/319/5867/1260#otherarticles>

This article appears in the following **subject collections**:

Neuroscience

<http://www.sciencemag.org/cgi/collection/neuroscience>

Information about obtaining **reprints** of this article or about obtaining **permission to reproduce this article** in whole or in part can be found at:

<http://www.sciencemag.org/about/permissions.dtl>

8. J. Y. Kwon, A. Dahanukar, L. A. Weiss, J. R. Carlson, *Proc. Natl. Acad. Sci. U.S.A.* **104**, 3574 (2007).
9. See supporting material on Science Online.
10. L. B. Vosshall, *Curr. Opin. Neurobiol.* **10**, 498 (2000).
11. K. S. Kosik, A. M. Krichevsky, *Neuron* **47**, 779 (2005).
12. A. Stark, J. Brennecke, R. B. Russell, S. M. Cohen, *PLoS Biol.* **1**, e60 (2003).
13. D. Grun, Y. L. Wang, D. Langenberger, K. C. Gunsalus, N. Rajewsky, *PLoS Comput. Biol.* **1**, e13 (2005).
14. A. Kuzin, T. Brody, A. W. Moore, W. F. Odenwald, *Dev. Biol.* **277**, 347 (2005).
15. B. P. Lewis, C. B. Burge, D. P. Bartel, *Cell* **120**, 15 (2005).
16. A. Couto, M. Alenius, B. J. Dickson, *Curr. Biol.* **15**, 1535 (2005).
17. S. Anton *et al.*, *Arthropod Struct. Dev.* **32**, 319 (2003).
18. P. Distler, J. Boeckh, *J. Exp. Biol.* **200**, 1873 (1997).
19. R. Ignell, T. Dekker, M. Ghaninia, B. S. Hansson, *J. Comp. Neurol.* **493**, 207 (2005).
20. F. J. Poelwijk, D. J. Kiviet, D. M. Weinreich, S. J. Tans, *Nature* **445**, 383 (2007).
21. We thank L. Vosshall, B. Dickson, W. Odenwald, R. Klein, G. Tavano, J. Carlson, and D. Anderson for providing reagents and comments on experiments; W. Tom, A. Lorenze, and P. Alcalá for technical assistance; A. Acker-Palmer, T. Suzuki, G. Tavano, R. Klein, and members of the laboratories for comments on the manuscript; A. Luke for helping with *miR-279* deletions; and Y.-T. Chou for cloning the luciferase sensors. Supported by the Jane Coffin Childs Memorial Fund and a National Research Service Award (P.C.); EMBO and

the Human Frontiers Science Program (I.G.K.); the Leukemia and Lymphoma Foundation, the Burroughs Wellcome Foundation, and the V-Foundation for Cancer Research (E.C.L.); and NIH grant DC006485 (S.L.Z.). G.S.B.S. is an HHMI Associate; S.L.Z. is an HHMI Investigator.

Supporting Online Material

www.sciencemag.org/cgi/content/full/319/5867/1256/DC1
Materials and Methods
Figs. S1 to S7
References

20 August 2007; accepted 17 January 2008
10.1126/science.1149483

Transgenic Inhibition of Synaptic Transmission Reveals Role of CA3 Output in Hippocampal Learning

Toshiaki Nakashiba, Jennie Z. Young, Thomas J. McHugh, Derek L. Buhl, Susumu Tonegawa*

The hippocampus is an area of the brain involved in learning and memory. It contains parallel excitatory pathways referred to as the trisynaptic pathway (which carries information as follows: entorhinal cortex → dentate gyrus → CA3 → CA1 → entorhinal cortex) and the monosynaptic pathway (entorhinal cortex → CA1 → entorhinal cortex). We developed a generally applicable tetanus toxin–based method for transgenic mice that permits inducible and reversible inhibition of synaptic transmission and applied it to the trisynaptic pathway while preserving transmission in the monosynaptic pathway. We found that synaptic output from CA3 in the trisynaptic pathway is dispensable and the short monosynaptic pathway is sufficient for incremental spatial learning. In contrast, the full trisynaptic pathway containing CA3 is required for rapid one-trial contextual learning, for pattern completion–based memory recall, and for spatial tuning of CA1 cells.

The medial temporal lobes of the brain, including the hippocampus, are crucial for learning and memory of events and space across species (1–3). The hippocampus receives input from virtually all associative areas of the neocortex via the entorhinal cortex (EC). In the main excitatory hippocampal network (Fig. 1A), information flows from the superficial layer (layer II) of the EC to the dentate gyrus (DG) to CA3 to CA1 and finally to the deep layers of EC directly or indirectly through the subiculum. This loop is referred to as the trisynaptic pathway (TSP). The hippocampus also contains a parallel excitatory monosynaptic pathway (MSP) [EC (layer III) → CA1 → EC (layer V)] as well as other excitatory and inhibitory circuits.

The prevailing view of the contribution of these circuits to hippocampal function (4–7) is that synaptic transmission and plasticity in the feed-forward pathway from EC → DG → CA3, a part of the TSP, are primarily responsible for pattern separation, whereas those in a recurrent

network within CA3 are crucial for the rapid association of diverse sets of information and pattern completion. Furthermore, CA1 may be instrumental in recognizing the novelty of an event or context (8, 9).

Some of these ideas have been tested by lesioning (10) portions of the hippocampus or EC, although it is difficult to restrict damage to specific subregions and cell types in a quantitative and reproducible manner (11, 12). These difficulties have in part been addressed by deleting the *N*-methyl-D-aspartate (NMDA) receptor gene *NR1* in specific hippocampal subregions with Cre-loxP recombination technology. These studies found that NMDA receptor–dependent synaptic plasticity in postnatal excitatory neurons of each of several hippocampal subregions is required for specific aspects of hippocampal learning and memory (13–16). In order to completely analyze hippocampal function, we developed a method to block neural transmission rather than synaptic plasticity and used it to assess the differential role of CA3 and EC outputs into area CA1 in hippocampus-dependent learning and memory.

We generated a triple transgenic mouse (Fig. 1B) by doxycycline (Dox)–inhibited circuit exocytosis knockdown (DICE-K), in which synaptic transmission is blocked by cell type–restricted and temporally controlled expression of the tet-

anus toxin (TeTX) light chain (17). TeTX is an endopeptidase specific for VAMP2 (18), which is essential for activity-dependent neurotransmitter release from presynaptic terminals (19). The rationale for this general method is described fully in the supporting online material (SOM).

We used the KA1 promoter (14) and α -CaMKII promoter (20) for the transgenic1 (Tg1) and transgenic2 (Tg2) mice, respectively, to block CA3 output in the TSP while keeping EC output in the MSP intact (Fig. 1B). Before generating the triple transgenic TeTX mouse line, we investigated several parameters of the DICE-K method by crossing the Tg1×Tg2 double transgenic mouse with a Tg3–green fluorescent protein (GFP) reporter line (CA3-GFP) (Fig. 1B). Immunohistology (Fig. 1, C to H) indicated that GFP expression was restricted to CA3 and DG in mice maintained on a Dox-free diet (Fig. 1, C to E). There was no expression of GFP in the CA1 pyramidal cell layer [stratum (s.) pyramidale] or temporoammonic (TA) pathway (s. lacunosum moleculare) but abundant expression in the Schaffer collateral (SC) pathway (s. radiatum and s. oriens) (Fig. 1E). In the Tg1×Tg2 mouse, the spatial restriction was much greater than in the Tg1 mouse (fig. S1). GFP expression was repressed in the Dox-on state (Fig. 1F), de-repressed in the Dox-on-off state (Fig. 1G), and re-repressed in the Dox-on-off-on state (Fig. 1H).

We crossed Tg1×Tg2 double transgenic mice with Tg3-TeTX mice to produce a triple transgenic mouse, CA3-TeTX. In hippocampal slices from control double transgenic mice (Tg1×Tg3-TeTX), VAMP2 immunoreactivity (IR) was observed where axonal terminals are known to exist (Fig. 1, I and M). Hippocampal VAMP2 IR patterns were indistinguishable between repressed CA3-TeTX and control mice (Fig. 1J). In hippocampal slices from CA3-TeTX mice that had been on Dox followed by 4 weeks of Dox withdrawal, there was a striking reduction of VAMP2 IR in the s. radiatum and s. oriens of CA1 and CA3 and in the inner one-third of the molecular layer (ML) of DG, but not in other strata (Fig. 1K). Similar patterns of VAMP2 IR were observed in hippocampal slices throughout the dorsoventral axis. The CA3-SC innervates CA1 in the s. radiatum and s. oriens, whereas CA3-recurrent collateral (RC) innervates CA3 in these

The Picower Institute for Learning and Memory, Howard Hughes Medical Institute, RIKEN-MIT Neuroscience Research Center, Department of Biology and Department of Brain and Cognitive Sciences, Massachusetts Institute of Technology, Cambridge, MA 02139, USA.

*To whom correspondence should be addressed. E-mail: tonegawa@mit.edu

strata. The inner one-third of ML is where mossy cells (MCs) innervate DG granule cells (21). Although the triple transgenic GFP mice showed moderate GFP IR in DG granule cells (Fig. 1G), there was no significant reduction of VAMP2 IR in the s. lucidum of CA3-TeTX mice where mossy fibers (MFs) from DG granule cells innervate CA3 (Fig. 1K). These results indicate that in the hippocampus of de-repressed CA3-TeTX mice, synaptic transmission should be impaired at SC-

CA1 synapses, at the CA3-RC synapses, and possibly at MC-DG granule cell synapses, but not at MF-CA3 synapses. There was no indication of VAMP2 IR reduction in the s. lacunosum moleculare where the TA axons synapse onto CA1 neurons, suggesting that TA synaptic transmission remained intact (Fig. 1K). In CA3-TeTX mice that underwent 3 weeks of Dox withdrawal followed by 7 weeks of Dox readministration, the VAMP2 IR distribution was similar to that in re-

pressed CA3-TeTX mice (Fig. 1J), indicating that TeTX-mediated blockade of synaptic transmission is reversible (Fig. 1L).

We characterized the input-output relationship of SC and TA inputs to a common population of postsynaptic CA1 neurons using extracellular field recordings. We found no significant genotype-specific effect on SC or TA inputs in repressed mice kept chronically on Dox (Fig. 2A). CA3-TeTX mice raised on Dox and shifted to Dox-off for 1, 2, 3, 4, or 6 weeks showed a sharp dropoff in synaptic transmission at SC inputs between 2 and 3 weeks after Dox withdrawal (fig. S2). At 4 weeks after Dox withdrawal, synaptic transmission was impaired at SC inputs but remained intact at TA inputs (Fig. 2B). Residual synaptic transmission at SC inputs in these mice failed to elicit population spikes in the field excitatory postsynaptic potential (fEPSP) at any stimulation intensity (Fig. 2, B and C insets, and table S2) or in response to high-frequency stimulation. Synaptic transmission at SC inputs was restored by a readministration of Dox for 6 weeks (Fig. 2C), confirming the reversibility of the DICE-K method. Based on these results, we used 4 weeks of Dox withdrawal (de-repressed mice) in most behavioral and in vivo electrophysiological studies. De-repressed CA3-TeTX mice exhibited no detectable abnormalities in the hippocampal cytoarchitecture (fig. S3) (22) or in locomotor activity, anxiety, motor coordination, or pain sensitivity (figs. S4 and S5).

We subjected de-repressed CA3-TeTX mice to the Morris water maze (MWM) task (16). The latency curves of these and control mice were indistinguishable (Fig. 3A) (see SOM for statistics of this and following experiments). Memory recall was tested by probe trials on days 6 and 11. On day 6, there was only a slight preference for the target quadrant (Fig. 3B) and the target platform location (Fig. 3, C and D) in both CA3-TeTX and control animals, and there was no difference between the two genotypes. On day 11, the preference was robust in both genotypes for both criteria (Fig. 3, B to D), but again there was no robust difference between genotypes.

To test a possible role of CA3 output in rapidly forming representation of a novel context in the hippocampus, we subjected CA3-TeTX mice to a contextual fear conditioning (CFC) task using a novel context. De-repressed CA3-TeTX mice exhibited less freezing than control littermates (Fig. 3, E and F). The context specificity of conditioning was comparable between genotypes (fig. S6A), as was the level of tone fear conditioning (fig. S6B). The freezing deficit observed while the mice were in the Dox-on-off state (fig. S7, C and D) was absent when the same mice were reconditioned in another chamber and tested after 6 weeks of Dox re-administration (Fig. 3, G and H), demonstrating the reversibility of the DICE-K method at the behavioral level. When the de-repressed CA3-TeTX mice were habituated to the chamber before receiving a foot shock, they still tended to freeze less than the control littermates,

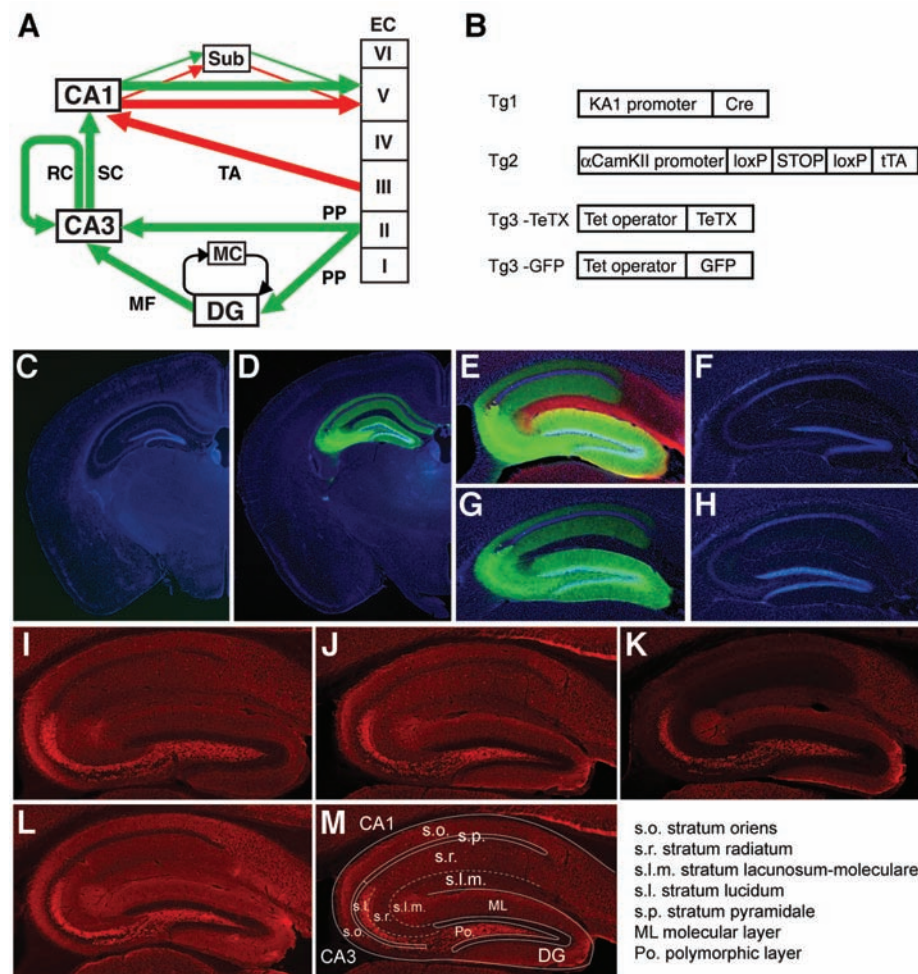


Fig. 1. Excitatory hippocampal-EC pathways and the DICE-K method applied to the TSP. (A) Excitatory pathways in the hippocampal formation and EC. Green and red arrows designate the TSP and MSP, respectively. Sub, subiculum; MC, mossy cells; PP, perforant pathway. (B) Tg1, a Cre transgenic line under control of the transcriptional regulator from the *kainate receptor 1* (*KA-1*) gene. Tg2, a tTA transgenic line under control of the α CaMKII promoter and Cre-loxP recombination. Tg3-TeTX and Tg3-GFP are TeTX and GFP transgenic lines, respectively, under control of the tetracycline (Tet) operator. (C and D) Double immunofluorescence staining of coronal sections from a Tg1xTg3-GFP control mouse (C) and chronically de-repressed CA3-GFP mouse (D) with antibodies specific for GFP (green) and for a cell nuclei marker, DAPI (blue). (E) Triple immunofluorescence staining of a hippocampal sagittal section from a chronically de-repressed CA3-GFP mouse with antibodies specific for GFP (green), DAPI (blue), and netrin-G1 (red, a marker for TA and lateral perforant axons) (34). The outer one-third of DG dendrites stain yellow because they are positive for both netrin-G1 (red) and GFP (green). (F to H) DAPI and GFP double staining of a hippocampal section from a chronically repressed CA3-GFP mouse (F), followed by 2 weeks of Dox withdrawal (G), followed by 2 weeks of Dox readministration (H). (I to L) Immunofluorescence staining with VAMP2 antibodies of a hippocampal section from control mice that have been on Dox diet (I). VAMP2 staining of a section from a CA3-TeTX littermate raised on a Dox diet (J) and after 4 weeks of Dox withdrawal (K) is shown. (L) A CA3-TeTX mouse having undergone 3 weeks of Dox withdrawal followed by 7 weeks of Dox readministration. (M) Locations of various hippocampal strata.

but the difference between the two genotypes was not significant (Fig. 3, I and J).

Our earlier study implicated NMDA receptor-dependent synaptic plasticity in CA3 pyramidal cells in pattern completion-based recall (14). To examine whether CA3 output in the TSP is crucial for this form of recall, we subjected CA3-TeTX mice to the pre-exposure mediated contextual fear conditioning (PECFC) paradigm (23, 24). De-repressed CA3-TeTX mice exhibited less freezing than control littermates, unlike repressed CA3-TeTX mice (fig. S8). To test whether de-repressed mice are defective in the recall phase, we habituated CA3-TeTX mice to the chamber under Dox-on conditions to ensure the formation of a contextual representation and then switched them to Dox-off conditions. Four weeks later, the animals were returned to the chamber for a 10-s exposure followed by a foot shock. CA3-TeTX mice displayed a deficit in freezing when tested on the following day (Fig. 3K), indicating that CA3 output in the TSP is crucial for pattern completion-based recall.

To investigate a possible role of CA3 output in the TSP in the detection and encoding of novel space, we recorded CA1 ensemble activity using multi-tetrode recordings (25) as freely moving mice completed 10 laps on a novel linear track (day 1). During this first experience, we observed a significant increase in the average firing rate of CA1 pyramidal cells in de-repressed CA3-TeTX mice, which accompanied a significant decrease in spatial tuning of these cells and spatial information (Fig. 4, A to E, and table S1). There were no differences in peak firing rate, bursting properties of these cells, or spike width (table S1). No differences were found in average firing rates of inhibitory interneurons recorded from CA3-TeTX and control littermates (table S1), suggesting that coding deficits are not due to a loss of feed-forward inhibition from CA3. The mice were then returned to the same linear track 24 (day 2) and 48 (day 3) hours after the initial exposure. Place fields remained larger and spatial information was less in CA3-TeTX mice than in controls (Fig. 4, A to E), indicating that CA3 output is crucial for spatial tuning not only on a novel but also a familiar track. Earlier work with CA3-lesioned rats reported a much milder impairment, if any, in a familiar environment (12). We found a decrease in place field size and average firing rate along with an increase in spatial information between days 1 and 2 in CA3-TeTX mice, whereas no difference was found between days in control mice (Fig. 4, A to E).

The spatial restriction and temporal control over the expression of the transgenic TeTX gene of the DICE-K method permit a greater degree of specificity in silencing neural pathways than is possible with traditional lesion or pharmacological methods. Several new genetic methods allow the inactivation or activation of specific neurons by manipulation of ligand- or light-activated cell-surface receptors or channels to permit rapid inactivation or activation of cells on

the subsecond-to-minute time scale. Hence, these are useful for studying relatively fast processes such as perception and short-term memory (26–30). In contrast, the kinetics of the DICE-K system are too slow for studying fast cognitive processes. Instead, this method can dissect the contribution of specific synaptic inputs to processes occurring over times from hours to weeks, such as intermediate- to long-term explicit memories and skill and habit learning. Because Dox can cross the blood-brain barrier, the DICE-K method can be used without complications from

direct continuous injections of impermeable ligands into the brain or invasive deep brain light delivery.

Our data show that CA3 output in the TSP is dispensable for both acquisition and recall of incremental spatial learning and memory recall in the MWM task. The nearly identical latency curves and probe trial behaviors of CA3-TeTX and control mice, along with the lack of thigmotactic behavior, indicate that CA3-TeTX mice indeed used an allocentric spatial strategy to locate the platform (Fig. 3D). Thus, it is likely

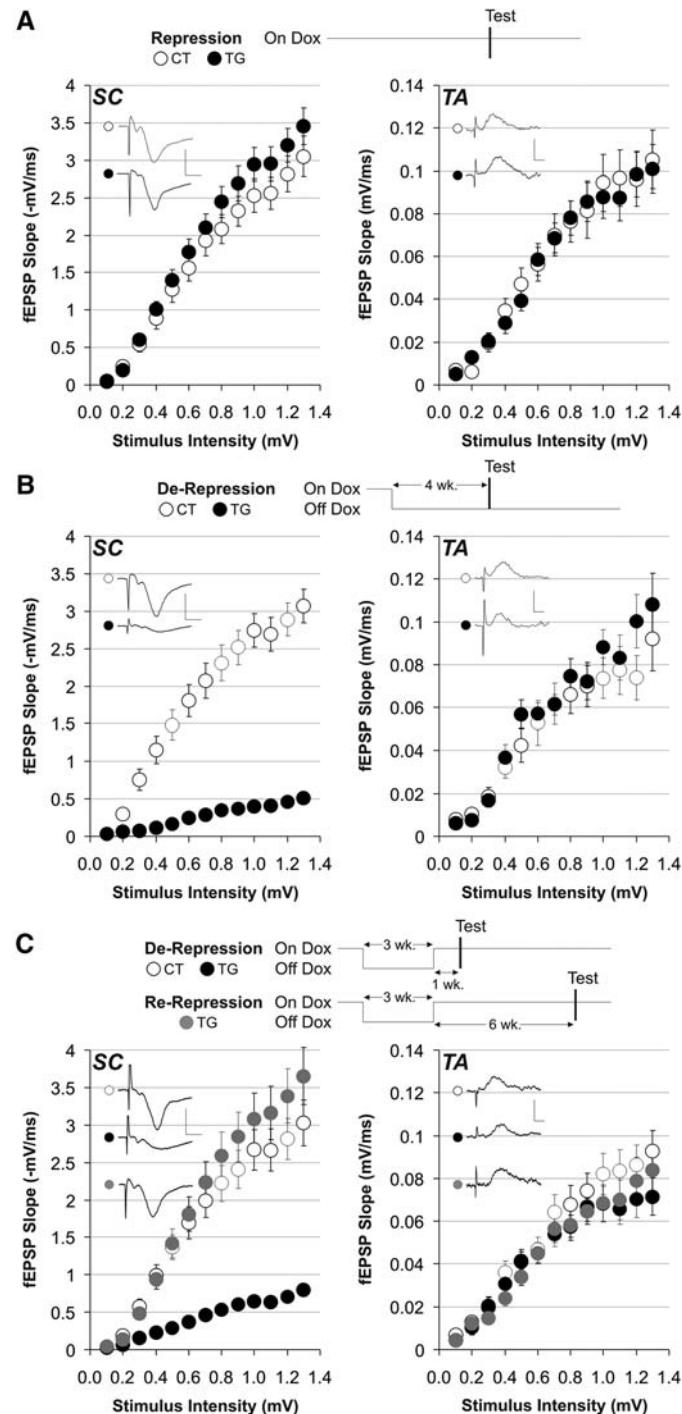


Fig. 2. Input-output relationships of SC and TA inputs to CA1 in CA3-TeTX (TG) mice and control littermates (CT). (A) Repressed (Dox-on) mice. (B) De-repressed (Dox on-off) mice after 4 weeks of Dox withdrawal. (C) De-repressed (Dox on-off: 3 + 1 week) and re-repressed (Dox on-off-on: 3 + 6 weeks) mice. Sample traces are representative of recorded mean maximal fEPSP slopes. Note the absence of population spikes in TG traces of (B) and (C). SC scale bar, 4 mV/2 ms; TA scale bar, 0.4 mV/4 ms. All statistics are given in the SOM.

Fig. 3. MWM and CFC. (A to D) Performance in MWM of CA3-TeTX (TG) and double transgenic (Tg1×Tg3-TeTX) control littermates (CT) having undergone 4 weeks of Dox withdrawal. (A) Averaged latencies. (B) Probe trials by relative quadrant occupancy time. (C) Numbers of platform crossings. Quadrant designations: TA, target; OP, opposite; L/R, left/right to target. (D) Heat maps of average search time during probe trials. (E and F) CFC in a novel context of de-repressed mice (4 weeks off Dox). (E) Kinetics of averaged freezing. (F) Freezing averaged over the 3-min test session. (G and H) CFC in a novel context of re-repressed mice (3 weeks off Dox followed by 6 weeks of Dox re-administration). (G) Kinetics of freezing. (H) Freezing averaged over the first 3-min test session. (I and J) CFC in de-repressed mice (4 weeks off Dox) after 3-day familiarization (10 min/day) with the conditioning chamber. (I) Kinetics of freezing. (J) Freezing averaged over the first 3-min session. (K) PECCF of mice having undergone Dox diet schedules indicated on top. Kinetics of averaged freezing (left) and reeizing averaged over the 5-min test session (right) are shown. CS, pre-exposure; US, foot shock. All statistics are given in the SOM.

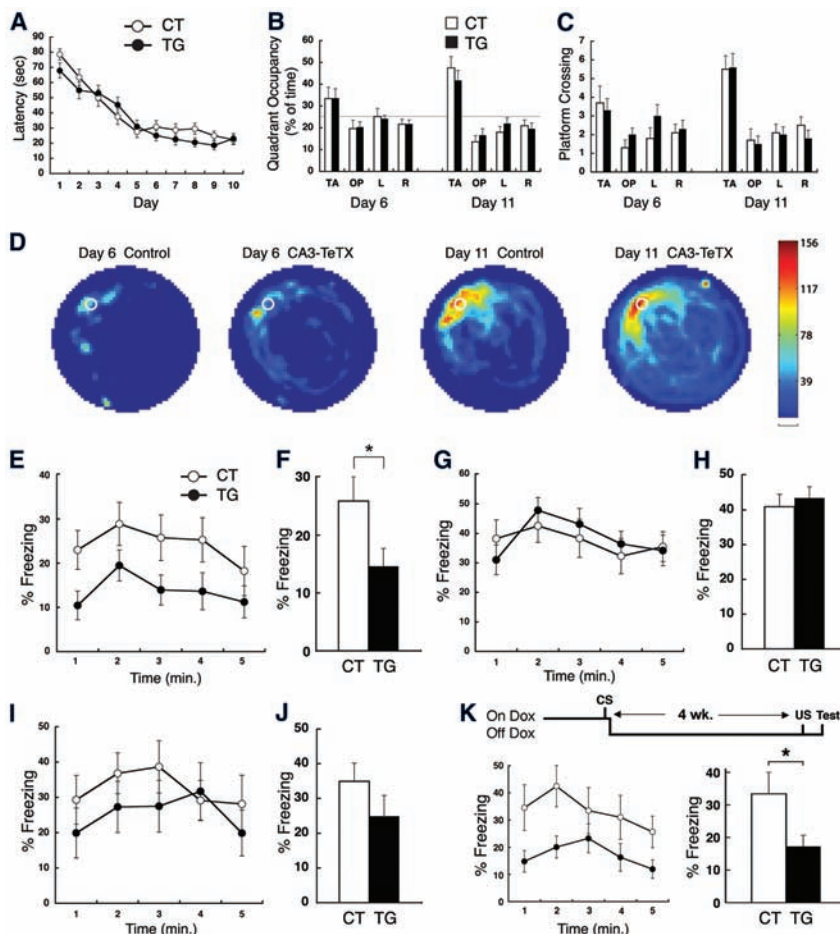
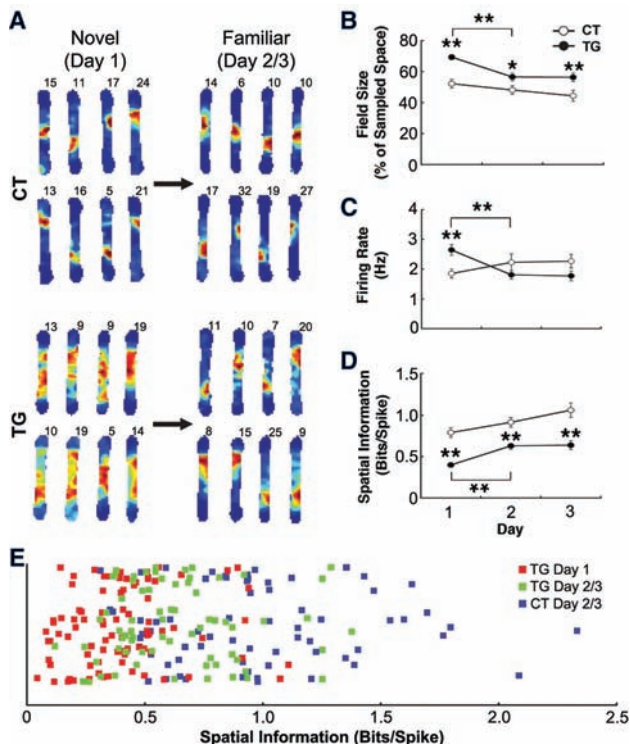


Fig. 4. CA1 place cells. (A) Representative examples of CA1 firing-rate maps in novel (day 1) and familiar (day 3) environments from CA3-TeTX (TG) mice and their double transgenic control littermates (CT) having undergone 4 weeks of Dox withdrawal, as mice completed 10 laps on a linear track. Colors are scaled to peak firing rates (in hertz) indicated at the top right of each map (blue, minimum; red, maximum). (B) Size of CA1 place fields, determined by the percentage of space where cells fire on the track for each day. (C) Average firing rate of all place cells plotted for each day. (D) Average spatial information (see SOM) for each day. (E) Spatial information for individual cells in novel (day 1) and familiar (day 3) environments. All statistics are given in the SOM. In (B) to (D), stars above solid circles indicate highly significant (**) or significant (*) differences between TG and CT. Double stars at the brackets indicate highly significant differences between TG day 1 and TG day 2.



that direct EC input to CA1 in the MSP can support these mnemonic processes. Our data contradict those of earlier studies conducted with rats with chemical or physical lesions, in which the integrity of CA3 or CA3 output was crucial for acquisition and/or recall in the MWM task (11, 12). Although this contradiction may be due to species or protocol differences, it is more likely a result of the greater specificity of our DICE-K method. Tuned spatial and navigational information is present in the superficial layers of EC, which may provide CA1 the necessary information for spatial learning (31, 32). Additionally, although CA1 neurons are poorly connected by recurrent collaterals, the MSP does form a closed loop EC III → CA1 → ECV → EC III (21) that may associate diverse spatial information, albeit less rapidly and less efficiently than the direct and robust recurrent network of CA3. Further, plasticity at MSP synapses of CA3-TeTX mice may mediate experience-dependent improvement in the MWM.

Our data also show that CA3 output is crucial for rapid one-trial learning in a novel context. It is thought that for CFC to occur, a representation of various contextual features must first be formed in the hippocampus and then must be conveyed to the amygdala via CA1 and/or the subiculum to be associated with the footshock representation (33). Evidently, the MSP cannot

provide these functions. The CFC deficit is reduced when animals are habituated to the context before the foot shock is delivered. Thus, with sufficient experience, the MSP seem to be able to fulfill a representation-forming and -conveying function.

Our *in vivo* recordings also illustrate a dichotomy between the ability of the TSP and MSP to support learning in novel and familiar space. The greatly reduced spatial tuning of CA1 pyramidal cells in CA3-TeTX mice on a novel track suggests that information contained in CA3 output is critical for rapid formation of a high-quality spatial representation and is consistent with the CFC deficit in a novel context. Further, the unexpectedly higher firing rates in CA3-TeTX mice under novel conditions suggests that in addition to providing spatial information, CA3 output may also help maintain appropriate levels of network excitability during novelty. On the other hand, the reduced deficit of spatial tuning during visits to the same track on days 2 and 3 indicates that the MSP alone can improve CA1 spatial tuning by experience, which is consistent with the reduced CFC deficit in a familiar context (Fig. 3, I and J) and the normal MWM performance (Fig. 3, A to D).

Thus, application of the DICE-K method to CA3 pyramidal cells demonstrates that the MSP (which bypasses CA3) can support slow incre-

mental learning in familiar environments but that the CA3 output of the TSP is needed for rapid acquisition of memories in novel environments and for pattern completion-based recall.

References and Notes

- W. B. Scoville, B. Milner, *J. Neuropsychiatry Clin. Neurosci.* **12**, 103 (1957).
- L. R. Squire, C. E. Stark, R. E. Clark, *Annu. Rev. Neurosci.* **27**, 279 (2004).
- L. E. Jarrard, *Behav. Neural Biol.* **60**, 9 (1993).
- D. Marr, *Philos. Trans. R. Soc. London Ser. B* **262**, 23 (1971).
- B. L. McNaughton, R. G. M. Morris, *Trends Neurosci.* **10**, 408 (1987).
- R. C. O'Reilly, J. L. McClelland, *Hippocampus* **4**, 661 (1994).
- J. L. McClelland, N. H. Goddard, *Hippocampus* **6**, 654 (1996).
- J. E. Lisman, N. A. Otmakhova, *Hippocampus* **11**, 551 (2001).
- D. Kumaran, E. A. Maguire, *Hippocampus* **17**, 735 (2007).
- E. T. Rolls, R. P. Kesner, *Prog. Neurobiol.* **79**, 1 (2006).
- B. Roozendaal *et al.*, *Nat. Neurosci.* **4**, 1169 (2001).
- V. H. Brun *et al.*, *Science* **296**, 2243 (2002).
- J. Z. Tsien, P. T. Huerta, S. Tonegawa, *Cell* **87**, 1327 (1996).
- K. Nakazawa *et al.*, *Science* **297**, 211 (2002).
- K. Nakazawa *et al.*, *Neuron* **38**, 305 (2003).
- T. J. McHugh *et al.*, *Science* **317**, 94 (2007).
- M. Yamamoto *et al.*, *J. Neurosci.* **23**, 6759 (2003).
- G. Schiavo *et al.*, *Nature* **359**, 832 (1992).
- S. Schoch *et al.*, *Science* **294**, 1117 (2001).
- M. Mayford *et al.*, *Science* **274**, 1678 (1996).
- M. P. Witter, D. G. Amaral, in *The Rat Nervous System*, G. Paxinos, Ed. (Academic Press, New York, 2004), pp. 635–710.
- K. J. Harms, A. M. Craig, *J. Comp. Neurol.* **490**, 72 (2005).
- M. S. Fanselow, *Anim. Learn. Behav.* **18**, 264 (1990).
- J. W. Rudy, R. C. O'Reilly, *Behav. Neurosci.* **113**, 867 (1999).
- M. A. Wilson, B. L. McNaughton, *Science* **261**, 1055 (1993).
- E. M. Tan *et al.*, *Neuron* **51**, 157 (2006).
- W. Lerchner *et al.*, *Neuron* **54**, 35 (2007).
- F. Zhang *et al.*, *Nature* **446**, 633 (2007).
- X. Han, E. S. Boyden, *PLoS One* **2**, e299 (2007).
- A. Y. Karpova, D. G. Tervo, N. W. Gray, K. Svoboda, *Neuron* **48**, 727 (2005).
- T. Hafting, M. Fyhn, S. Molden, M. B. Moser, E. I. Moser, *Nature* **436**, 801 (2005).
- F. Sargolini *et al.*, *Science* **312**, 758 (2006).
- S. Maren, *Annu. Rev. Neurosci.* **24**, 897 (2001).
- S. Nishimura-Akiyoshi, K. Niimi, T. Nakashiba, S. Itohara, *Proc. Natl. Acad. Sci. U.S.A.* **104**, 14801 (2007).
- We thank F. Bushard, C. Carr, X. Zhou, J. Derwin, A. Ogawa, C. Lovett, and M. Ragion for technical assistance; N. Arzumanyan for her help in manuscript preparation; and A. Govindarajan, S. Itohara, M. Remondes, M. Wilson, and members of the Tonegawa lab for advice and discussion. Supported by NIH grants R01-MH078821 and P50-MH58880 to S.T.

Supporting Online Material

www.sciencemag.org/cgi/content/full/1151120/DC1
Materials and Methods
SOM Text
Figs. S1 to S8
Tables S1 and S2
References

28 September 2007; accepted 11 January 2008
Published online 24 January 2008;
10.1126/science.1151120
Include this information when citing this paper.

BOLD Responses Reflecting Dopaminergic Signals in the Human Ventral Tegmental Area

Kimberlee D'Ardenne,^{1,2*} Samuel M. McClure,^{2,3} Leigh E. Nystrom,^{2,3} Jonathan D. Cohen^{2,3,4}

Current theories hypothesize that dopamine neuronal firing encodes reward prediction errors. Although studies in nonhuman species provide direct support for this theory, functional magnetic resonance imaging (fMRI) studies in humans have focused on brain areas targeted by dopamine neurons [ventral striatum (VStr)] rather than on brainstem dopaminergic nuclei [ventral tegmental area (VTA) and substantia nigra]. We used fMRI tailored to directly image the brainstem. When primary rewards were used in an experiment, the VTA blood oxygen level-dependent (BOLD) response reflected a positive reward prediction error, whereas the VStr encoded positive and negative reward prediction errors. When monetary gains and losses were used, VTA BOLD responses reflected positive reward prediction errors modulated by the probability of winning. We detected no significant VTA BOLD response to nonrewarding events.

Functional magnetic resonance imaging (fMRI) has become a prominent method for imaging brain activity in humans. Commonly used fMRI protocols acquire functional data with a spatial resolution on the order of several millimeters. These protocols are adequate for measuring blood oxygen level-dependent (BOLD) responses from relatively large neural structures such as the cortex and basal ganglia. However, they are not suitable for imaging brain-

stem structures that are of long-standing interest to neuroscientists. In particular, the brainstem nuclei of the dopamine, norepinephrine, and serotonin systems have long been known to play a critical role in the regulation of brain function, and disturbances of these systems have been implicated in most major psychiatric disorders. Recent theoretical advances have begun to identify specific functions for these brainstem systems. In particular, the reward prediction error

theory of dopamine function (1, 2) proposes a role for this neuromodulator in reinforcement learning. This theory makes specific predictions that have been tested in direct neuronal recordings from brainstem dopaminergic nuclei in nonhuman species. However, imaging studies in humans have been restricted to measurements from projection areas of the dopamine system [such as the ventral striatum (VStr) and medial prefrontal cortex] that are larger and therefore more easily imaged with fMRI. Here, we report the use of a combination of recently developed neuroimaging techniques that address the difficulties inherent to brainstem imaging in order to directly image the VTA.

There are several methodological challenges to imaging brainstem nuclei. First among them is the small size of the nuclei. The VTA is ~60 mm³ in volume (3), or roughly the size of 2 voxels at the resolution common in fMRI studies (4–18). To address this issue, we acquired high-resolution echo planar images that have been shown to be sufficient to discern individual subcortical nuclei

¹Department of Chemistry, Princeton University, Princeton, NJ 08544, USA. ²Center for the Study of Brain, Mind, and Behavior, Princeton University, Princeton, NJ 08544, USA. ³Department of Psychology, Princeton University, Princeton, NJ 08544, USA. ⁴Department of Psychiatry, University of Pittsburgh, Pittsburgh, PA 15260, USA.

*To whom correspondence should be addressed. E-mail: dardenne@princeton.edu